

Theory of phase-adaptive parametric cooling

Alekhya Ghosh^{1,2}, Pardeep Kumar¹, Christian Sommer,³ Fidel G. Jimenez⁴,
 Vivishek Sudhir^{5,6} and Claudiu Genes^{1,2}

¹Max Planck Institute for the Science of Light, Staudtstraße 2, D-91058 Erlangen, Germany

²Department of Physics, Friedrich-Alexander-Universität Erlangen-Nürnberg, Staudtstraße 7, D-91058 Erlangen, Germany

³AQT, Technikerstraße 17, 6020, Austria

⁴Pontificia Universidad Católica del Perú, Av. Universitaria 1801, San Miguel 15088, Peru

⁵LIGO Laboratory, Massachusetts Institute of Technology, Cambridge, Massachusetts 02139, USA

⁶Department of Mechanical Engineering, Massachusetts Institute of Technology, Cambridge, Massachusetts 02139, USA



(Received 27 May 2022; accepted 10 May 2023; published 30 May 2023)

We propose an adaptive phase technique for the parametric cooling of mechanical oscillators. Our scheme calls for a sequence of periodic adjustments of the phase of a parametric modulation of the mechanical oscillator that is conditioned on measurements of its two quadratures. The technique indicates an exponential loss of thermal energy at initial high occupancies, similar in performance to other optomechanical techniques such as cold-damping or cavity self-cooling. As the quantum ground state is approached, the phase adaptive scheme leads to residual occupancies at the level of a few phonons owing to the competition between parametric amplification of quantum fluctuations and the feedback action.

DOI: [10.1103/PhysRevA.107.053521](https://doi.org/10.1103/PhysRevA.107.053521)

I. INTRODUCTION

Mechanical resonators are oftentimes used in displacement [1], force [2], acceleration [3], or mass sensing [4] applications. Bringing them to their quantum ground state is of fundamental interest for research studying the classical to quantum physics transition [5–8]. A particularly successful approach has been through the radiation-pressure coupling between motion and light in the field of cavity optomechanics [9]. Cooling close to the quantum ground state of an isolated mechanical resonance has been achieved both via cavity self-cooling [10–13] and active feedback [14–19]. In the second case, detection of the light scattered from an optomechanical system allows for the implementation of a cold-damping mechanism [20], where a viscous force proportional to the momentum is provided. Extensions to the simultaneous feedback cooling of many mechanical resonances are also possible [21,22]. Both these two paths were extensively utilized theoretically and experimentally and their advantages and limitations are well understood [9,23,24]. More recently, a third option, dubbed parametric cooling, has arisen as an efficient option for cooling optically levitated particles [25,26], atoms in cavities [27], or nanoelectromechanical resonators [28]. For a generic oscillator at resonance frequency Ω , the main ingredient of this technique is the periodic modulation of the spring constant at 2Ω . In the particular

case of levitated nanoparticles, this is achieved by feedback control of the trapping potential [29]. The cooling mechanism is then similar to cold-damping but with a nonexponential loss rate of energy [25,30].

Here, we propose a variation of the parametric cooling technique, which is not based on a controlled cold-damping feedback loop [17], but instead on the adjustment of the modulation phase, similarly to the variation of the angle of a squeezing operation in the case of trapped ions [31]: we dub this technique *phase adaptive parametric cooling*. The technique solely requires the detection of the momentum and position quadratures of the oscillator from which an optimal modulation phase is deduced and fed back into the system (as illustrated in Fig. 1). Parametric driving of an oscillator of

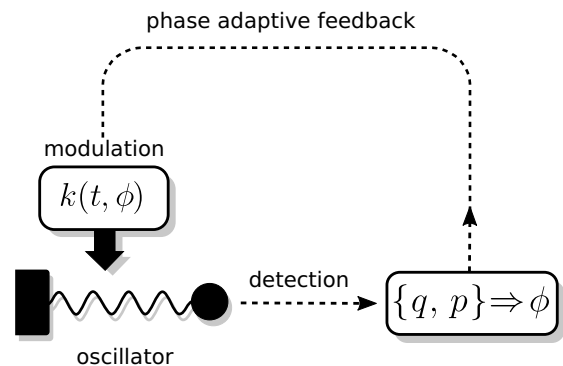


FIG. 1. Parametric cooling via phase adaptive feedback. Generic oscillator with natural frequency Ω . Detection of the mechanical quadratures q and p allows for the design of an adaptive phase feedback strategy, based on the parametric modulation of the spring constant at frequency 2Ω and adjustable modulation phase ϕ .

Published by the American Physical Society under the terms of the [Creative Commons Attribution 4.0 International](https://creativecommons.org/licenses/by/4.0/) license. Further distribution of this work must maintain attribution to the author(s) and the published article's title, journal citation, and DOI. Open access publication funded by the Max Planck Society.

displacement x with natural frequency Ω and mass m consists in supplementing the bare restoring force $\mathcal{F} = -m\Omega^2 x$ with an extra small modulation $\delta\mathcal{F} = 2m\Gamma\Omega \cos(2\Omega t + \phi)x$ (under the condition $\Gamma \ll \Omega$). Alternatively, this can be understood as a periodic and phase-dependent variation of the spring constant $k(t, \phi)$.

The key point in our treatment is the observation that the phase ϕ is a crucial tuning knob: when properly adjusted, it can lead to an exponential loss of energy at rate Γ . An optimal phase ϕ_{opt} , to be fed back into the modulation intensity, is derived from the detected quadratures, hence it is subject to any imprecision occurring in the measurement process as well as, most importantly, to the intrinsic quantum uncertainty. In the absence of any measurement imprecision, for a thermal environment at average occupancy $n_{\text{th}} \gg 1$, a final occupancy as low as $\gamma n_{\text{th}}/\Gamma$ can be reached, where γ is the intrinsic mechanical damping. Quantum fluctuations in the intrinsic position and momentum are negligible at high occupancies since, in this ‘‘classical’’ regime, the quadratures have a large mean value and so the cooling rate is well quantified by Γ . As the ‘‘quantum’’ regime of low occupancy is approached, quantum fluctuations of the detected quadratures play a crucial role. In particular, parametric modulation amplifies quantum fluctuations of the quadratures. However, our phase adaptive feedback technique inhibits such an amplification of the quantum noise and rather competes with it to provide a nonzero residual occupation at the level of a few phonons.

The paper is organized as follows. In Sec. II we introduce the model for the quantum mechanical oscillator subject to a parametrically modulated restoring force and to quantum thermal noise. In Sec. III we derive the conditions where a cooling solution emerges as a function of the modulation phase and show how feedback can be implemented to optimize the cooling behavior. We extend our analytical and numerical treatment to the question of thermally activated resonators and find limits for the residual occupancy and analyze the effect of measurement imprecision and the question of multimode cooling in Sec. IV. We finally address the question of quantum ground-state cooling in Sec. V and present further discussions and conclusions in Sec. VI.

II. MODEL AND EQUATIONS

We consider a mechanical resonance along some quantized direction \hat{x} of mass m subjected to the standard restoring force $\mathcal{F} = -m\Omega^2 \hat{x}$, where Ω is the natural oscillation frequency. In addition, we consider an extra, weak parametric modulation

$$\delta\mathcal{F} = 2m\Gamma\Omega \cos(2\Omega t + \phi)\hat{x}, \quad (1)$$

with modulation amplitude $\Gamma \ll \Omega$ and phase ϕ . Using the definition of the zero point motional amplitude $x_{\text{zpm}} = \sqrt{\hbar/(2m\Omega)}$, we can introduce the dimensionless position $\hat{q} = \hat{x}/x_{\text{zpm}}$ and its associated momentum quadrature \hat{p} with the usual commutation relation $[\hat{q}, \hat{p}] = i$. Heisenberg-Langevin equations for the dimensionless quadratures can be derived from the expression of the two forces listed above, which read

$$\frac{d\hat{q}}{dt} = \Omega\hat{p}, \quad (2a)$$

$$\frac{d\hat{p}}{dt} = -\gamma\hat{p} - \Omega\hat{q} + 2\Gamma \cos(2\Omega t + \phi)\hat{q} + \hat{\zeta}(t). \quad (2b)$$

In the absence of the external modulation force $\delta\mathcal{F}$, the mode is in equilibrium with a bath at temperature T_{th} to which an average occupancy n_{th} corresponds. The action of the bath onto the mechanical resonance is modeled via noise operators $\hat{\zeta}(t)$ of zero average and with two time correlations

$$\langle \hat{\zeta}(t)\hat{\zeta}(t') \rangle = \frac{1}{2\pi} \int d\omega S_{\zeta}(\omega) e^{-i\omega(t-t')}. \quad (3)$$

The thermal power spectrum is given by the following expression:

$$S_{\zeta}(\omega) = \frac{\gamma\omega}{\Omega} \left\{ \coth \left[\frac{\hbar\omega}{2k_B T_{\text{th}}} \right] + 1 \right\}. \quad (4)$$

Notice that an equivalent approach, based on canonical noise equally affecting both quadratures, could be taken (as detailed in Appendix D) as long as $n_{\text{th}} \gg 1$, which is usually the case in optomechanics [23,32,33]. For large mechanical quality factors $\mathcal{Q}_m = \Omega/\gamma \gg 1$ some simplifications can be performed which lead to simple expressions for both the thermal damping rate, defined in terms of sidebands $\gamma = [S_{\zeta}(\Omega) - S_{\zeta}(-\Omega)]/2$ and for the average thermal occupancy $n_{\text{th}} = [S_{\zeta}(\Omega) + S_{\zeta}(-\Omega)]/(2\gamma)$. Notice that the equipartition theorem implies that, in a thermal state, the variance in the two quadrature is the same and derivable as $\langle \hat{q}^2 \rangle = \langle \hat{p}^2 \rangle = n_{\text{th}} + 1/2$.

The task in the following is to study the classical and quantum behavior of such an oscillator under the combined action of the thermal bath and of the parametric modulation. To this end we will first address the classical problem in the following two sections and relegate the question of quantum ground state cooling to Sec. V.

III. ADAPTIVE PHASE COOLING

In a first step, we take an average over the Langevin equations and construct a second-order differential equation for the expectation value $q = \langle \hat{q} \rangle$. We then follow a perturbative method requiring that the modulation parameter $b = \Gamma/\Omega \ll 1$ is small. Eliminating the trivial exponential damping with $q = \bar{q}e^{-\gamma t/2}$ allows for the derivation of a Mathieu-like equation

$$\ddot{\bar{q}} + [\Omega'^2 - 2b\Omega'^2 \cos(2\Omega t + \phi)]\bar{q} = 0, \quad (5)$$

where $\Omega' = \sqrt{\Omega^2 - \gamma^2/4}$ (as $\mathcal{Q}_m \gg 1$, one can safely approximate this term in the following with Ω). Further simplifications are obtained via the transformation to a dimensionless time variable $\bar{t} = \Omega t + \phi/2$. The dynamics can now be exactly mapped onto the standard Mathieu equation

$$\frac{d^2 q_M}{d\bar{t}^2} + [1 - 2b \cos(2\bar{t})]q_M = 0. \quad (6)$$

Notice that in above formalism, the reverse transformation from \bar{t} to the real time variable is then done via $q(t) = q_M(\Omega t + \phi/2)e^{-\gamma t/2}$.

A. Perturbative solution

The standard solution to Eq. (6) can be written as an infinite sum of harmonics

$$q_M(\bar{t}) = \mathcal{E}_- e^{i\beta\bar{t}} \sum_{n=-\infty}^{n=\infty} C_{2n} e^{i2n\bar{t}} + \mathcal{E}_+ e^{-i\beta\bar{t}} \sum_{n=-\infty}^{n=\infty} C_{2n} e^{-i2n\bar{t}}, \quad (7)$$

where the coefficients β and C_{2n} are found by replacing the solution back in Eq. (6). This leads to (see Ref. [31]) a recursive equation

$$C_{2n+2} - D_{2n}C_{2n} + C_{2n-2} = 0, \quad (8)$$

where

$$D_{2n} = \frac{1 - (2n + \beta)^2}{b}. \quad (9)$$

In the limit of small b , the first three terms in the expansion above suffice to properly describe the trajectory: we reduce the analysis to $n = 0, \pm 1$. For $\beta = -1 + x$, where x is a complex number with amplitude much smaller than unity, we find that $D_0 = 2x/b$ and $D_2 = -2x/b$ while all other D s are very large. Fixing (without loss of generality) $C_0 = 1$ and truncating all coefficients for $|n| > 1$ we obtain $x = ib$ and $C_2 = i$, as the only nonvanishing coefficient.

We can now show that, to a very good approximation, the solution can be written in terms of negative and positive damping components

$$q(t) = \mathcal{A}_- e^{-\frac{(\gamma+\Gamma)t}{2}} \cos(\Omega t + \phi') + \mathcal{A}_+ e^{-\frac{(\gamma-\Gamma)t}{2}} \sin(\Omega t + \phi'), \quad (10)$$

where we rewrite the following coefficients in a more concise way (so that they become real) $\mathcal{A}_- = 2\mathcal{E}_- e^{i\pi/4} e^{-b\phi/4}$ and $\mathcal{A}_+ = 2\mathcal{E}_+ e^{i\pi/4} e^{b\phi/4}$ and the newly introduced phase is $\phi' = \phi/2 + \pi/4$. This shows the occurrence of an additional optical damping rate Γ (we assume $b > 0$) that adds to the intrinsic thermal damping γ . The negative solution indicates increased damping, while the positive solution leads to a heating instability as soon as Γ becomes larger than γ .

The coefficients \mathcal{E}_\pm are derived from the initial conditions q_0 and p_0 and their ratio strongly depends on the driving phase ϕ . The initial conditions ask that $q_M(\bar{t} = \frac{\phi}{2}) = q(t=0) = q_0$ and $\dot{q}_M(\bar{t} = \frac{\phi}{2}) = p(t=0) = p_0$, which leads to the following set of equations:

$$\mathcal{A}_- \cos \phi' + \mathcal{A}_+ \sin \phi' = q_0, \quad (11a)$$

$$-\mathcal{A}_- \sin \phi' + \mathcal{A}_+ \cos \phi' - \frac{b}{2} \mathcal{A}_- \cos \phi' + \frac{b}{2} \mathcal{A}_+ \sin \phi' = p_0. \quad (11b)$$

In a first step, we neglect \mathcal{A}_+ assuming it is much smaller than the damped solution and obtain from above

$$\phi_{\text{opt}}^{(0)} = \frac{\pi}{2} + 2 \tan^{-1} \left[\frac{1}{\frac{p_0}{q_0} + \frac{b}{2}} \right]. \quad (12)$$

Fixing the modulation phase to the optimal value listed above means that the system will follow a cooling dynamics in the initial stages. In the long time limit, independently of the initial conditions, the system will blow up as the heating solution always prevails owing to the rise with time in the exponential term. For the chosen optimal phase, the signs of the sin and cos terms are always the same, which leads to $|\mathcal{A}_-| = \sqrt{q_0^2 + p_0^2}$ thus equal to the initial variance of the thermal state.

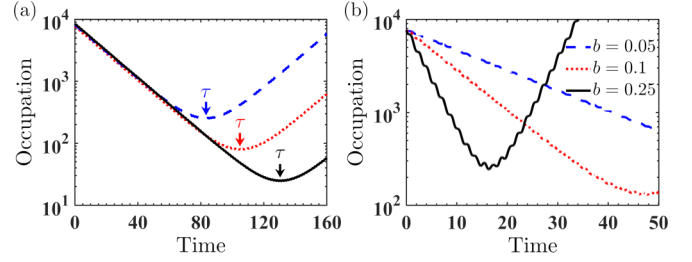


FIG. 2. Single shot cooling. (a) Occupancy for three randomly selected initial conditions ($q_0^{(j)}, p_0^{(j)}$) for $j = 1, 2, 3$ (adding to the same initial energy), each with an optimized phase $\phi_0^{(j)}$. All trajectories show exponential cooling up to the turning points τ_j where the damped solution is comparable to the growing one. The parameters are $\gamma/\Omega = 10^{-6}$, $n_{\text{th}} = 10^4$, and $b = 0.05$. The time is in inverse units of Ω . (b) Time dynamics of the occupancy for increasing values of b [other parameters same as in (a)]. Higher values of b lead to faster cooling.

B. Optimal modulation phase and feedback

Let us now simplify the above derivation and stress again that the important condition is that $\mathcal{A}_- \gg \mathcal{A}_+$, which allows for the damped solution to dominate at early times. For $b \ll 1$, we can verify numerically that even a more simplified analytical expression can be found for the optimal phase as

$$\phi_{\text{opt}}^{(0)} = \frac{\pi}{2} + 2 \tan^{-1} \left[\frac{q_0}{p_0} \right]. \quad (13)$$

This expression allows us to formulate the strategy for the single-shot cooling mechanism. This involves the detection of the initial conditions which then is followed by the optimization of the modulation phase. The resulting cooling occurs for any initial conditions as illustrated in Fig. 2. The loss of energy is exponential at the analytically predicted rate Γ and dominates up to a time τ where (roughly) $\tau \approx (1/\Gamma) \ln(\mathcal{A}_-/\mathcal{A}_+)$ (where the positive and negative solutions are comparable). This means that the occupancy reached at time τ is roughly $\mathcal{A}_-/\mathcal{A}_+$ times smaller than the initial one.

The above illustration already suggests the mechanism to achieve control over the cooling dynamics at arbitrarily long times: at regular times $j\delta\tau$ (with $j = 1, \dots, N$ and the repetition time interval $\delta\tau < \tau$), before heating starts to dominate, we detect the instantaneous values of $q(j\delta\tau)$ and $p(j\delta\tau)$ and update the phases $\phi(j\delta\tau)$ to the values indicated by Eq. (13). Following this procedure for N steps suggests the loss of energy roughly by a factor of $1/b^N$. For values of b around 0.1, in only six feedback steps we can reduce an initial $n_{\text{th}} = 10^4$ average occupancy to well below unity, as described below.

IV. CLASSICAL FEEDBACK COOLING LIMITS

The previous section shows that the initial choice of the modulation phase combined with a repeated resetting of the phase extracted from the detection of the quadratures leads to efficient exponential cooling dynamics. Let us now analyze the performance of this technique in the presence of thermal noise and measurement imprecision. Also, we extend here the mechanism to the question of simultaneous cooling of a few distinct resonances.

A. Inclusion of thermal noise

Let us consider the action of classical thermal noise, under the Markovian approximation, modeled as a Wiener process $dW(t)$ of zero average and variance $dW(t)^2 = dt$. To this end we write the following set of coupled difference equations:

$$dq = \Omega p dt, \quad (14a)$$

$$dp = -\gamma p dt - \Omega q dt + \mathcal{F}_{\text{mod}} dt + \sqrt{2\gamma n_{\text{th}}} dW(t). \quad (14b)$$

We can easily check that, in the absence of the trap modulation force, the system thermalizes, as expected, at rate γ to the environmental temperature T_{th} (occupancy n_{th}) (see Appendix A). Numerically, we can model the Wiener increment [34] in terms of a normal distribution such that $dW(t) = \sqrt{dt} \mathcal{N}(0, 1)$, where $\mathcal{N}(0, 1)$ describes a normally distributed random variable of unit variance. A semi-analytical solution can be instead found by turning the difference equations into a set of recurrence equations (see Appendix B). We discretize the time interval $[0, t]$ into n steps of duration $dt = t/n$. The equations above can be rewritten as $\mathbf{v}_n - \mathcal{M}_n \mathbf{v}_{n-1} = \sqrt{2\gamma n_{\text{th}}} \mathbf{u} dW_n$ where $\mathbf{v} = (q, p)^T$ and $\mathbf{u} = (0, 1)^T$ and the evolution matrix is defined as

$$\mathcal{M}_n = \begin{bmatrix} 1 & \Omega dt \\ -\Omega dt + 2\Gamma \cos[2\Omega(n-1)dt + \phi] dt & 1 - \gamma dt \end{bmatrix}. \quad (15)$$

A formal analytical solution can be written in terms of time ordered matrices $\mathcal{T}_{n_j} = \mathcal{M}_n \mathcal{M}_{n-1} \dots \mathcal{M}_j$ in the following form:

$$\mathbf{v}_n = \mathcal{T}_{n1} \mathbf{v}_0 + \sqrt{2\gamma n_{\text{th}}} \sum_{j=1}^{n-1} \mathcal{T}_{nj} \mathbf{u} dW_{n-j}. \quad (16)$$

The first part in the equation above is the deterministic evolution from the initial conditions, while the last part is the long-term behavior dominated by thermal noise. Notice that for $n_{\text{th}} = 0$, the evolution matrix is time independent and the \mathcal{T}_{n_j} is simply equal to $\mathcal{M}^{(n-j)}$ which allows for analytical solutions. The phase adaptive feedback algorithm is then as chosen as follows: at $t = 0$, the modulation phase is picked at $\phi_{\text{opt}}^{(0)}$ to ensure an initial damping period. Monitoring of q and p at regular time intervals $j\delta\tau$ (with $j = 1, \dots, N$) is then followed by an update of the modulation phases $\phi_{\text{opt}}^{(j)}$ fixed by Eq. (13) with the replacement of the instantaneous quadratures $q_j = q(j\delta\tau)$ and $p_j = p(j\delta\tau)$. In Fig. 3(a), the performance of the technique is exemplified on three different trajectories (in the absence of noise) with identical initial conditions but different feedback times. For an optimized $\phi_{\text{opt}}^{(0)}$, the red line shows the heating in the absence of feedback, while a slow feedback ($\delta\tau > \tau$) leads to regions of heating and cooling (magenta line). Perfectly exponential loss is reached for quick feedback with $\delta\tau < \tau$ (blue line). In Fig. 3(b), in the presence of thermal noise, two randomized trajectories show the same cooling rate (at rate Γ) and the same final occupancy. From equilibrium considerations [23], the final occupancy can be deduced as the ratio of the reheating rate of the ground state γn_{th} and the total damping rate $\gamma + \Gamma$

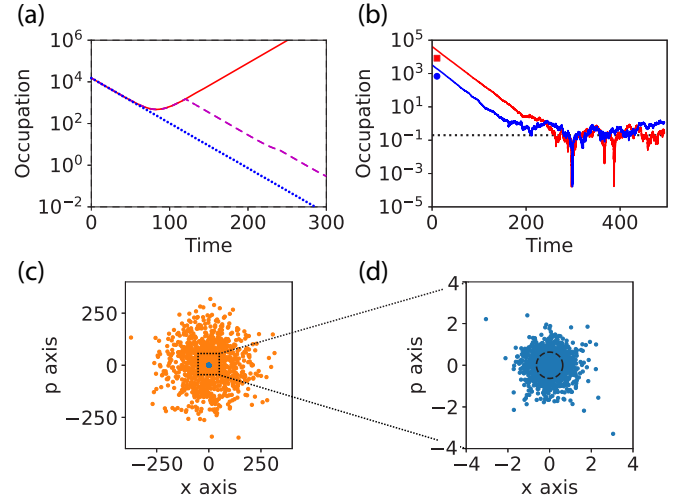


FIG. 3. Feedback phase adaptive cooling. (a) Occupancy for a given set of initial conditions with the same energy, assuming initially fixed phase (red, full line) as opposed to adapted phase with $\delta\tau < \tau$ (blue line, dotted, fast feedback) and $\delta\tau > \tau$ (magenta line, dashed, slow delayed feedback). (b) Two trajectories with different initial conditions randomly picked from a thermal distribution with $n_{\text{th}} = 10^4$. The initial exponential cooling saturates close to the ground state as the competition between Brownian noise thermal heating and parametric cooling shows the reach of an equilibrium final occupancy at $n_{\text{final}} \approx \gamma n_{\text{th}} / \Gamma$. (c) Phase-space illustration of an initial thermal state (10^3 points in orange) and the corresponding final cold state (in blue). (d) Zoom-in of the final occupancy distribution showing a thermal distribution. The parameters are $\gamma/\Omega = 10^{-6}$ and $b = 0.05$. Time is expressed in inverse units of Ω .

such that $n_{\text{final}} = \gamma n_{\text{th}} / (\gamma + \Gamma)$. Figures 3(c) and 3(d) show that both the initial and final states are thermal.

B. Measurement imprecision

Consider now the case of imperfect detection, when the detected phase ϕ_{opt} is uncertain up to a value $\delta\phi$ of zero average with variance σ_ϕ . This stems from the imprecision in the detection of the quadratures with an expression that can be directly deduced by applying the error propagation formula to Eq. (13). Let us model the measurement imprecision by taking a classical stochastic average over Eq. (2) such that the modulation term $2\Gamma \cos(2\Omega t + \phi + \delta\phi) \hat{q}$ becomes a stochastic force. We then expand it in terms of exponentials and then make use of the property of any Gaussian noise that $\langle e^{i\delta\phi} \rangle_{\text{cl}} = e^{-(\delta\phi^2)_{\text{cl}}}$ where the bracket signifies a classical averaging over many realizations. The force modulation, averaged, then reads $2\Gamma e^{-\sigma_\phi} \cos(2\Omega t + \phi) \hat{q}$, showing that the measurement uncertainty simply leads to the rescaling of the effective cooling rate from Γ to $\Gamma e^{-\sigma_\phi}$.

Sample trajectories simulating imperfect detection are shown in Fig. 4(a) for a normal distribution of width $\sigma_\phi = 0.3$. The average over trajectories then fits perfectly to the derived analytical result showing the progressive reduction of the cooling rate with increasing measurement imprecision as is apparent from the slope of the lines in Fig. 4(b).

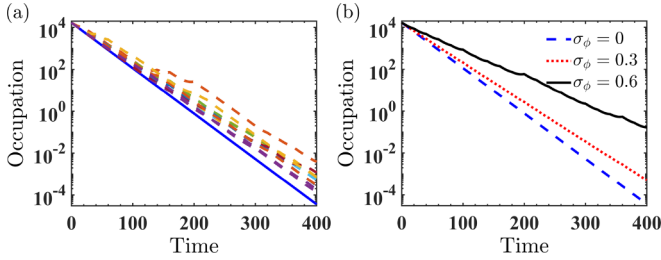


FIG. 4. Influence of the measurement imprecision. (a) Sample trajectories (dashed lines) obtained from the imperfect detection producing uncertainty in the phase which is modeled by a Gaussian distribution of width $\sigma_\phi = 0.3$. Occupancy without measurement imprecision is shown as a reference (solid blue line). (b) Average occupancy for different widths of the phase distributions. Parameters used are $\gamma/\Omega = 10^{-6}$, $b = 0.05$, and $n_{\text{th}} = 10^4$. Here time is expressed in inverse units of Ω and occupancy is obtained for an adapted phase with $\delta\tau < \tau$. The slopes of the occupancy curves fit very well to the analytical prediction.

C. Simultaneous cooling

Interestingly, the above phase adaptive mechanism can be extended to simultaneously cool a number n_{res} of adjacent mechanical resonances as previously tackled via other cooling techniques [35–37]. This scenario can refer to either a number of different vibrations of a single resonator or to the case of many levitated particles within the same optical trap (for different particle size a different oscillation frequency is obtained). Let us denote these frequencies by Ω_k with $k = 1, \dots, n_{\text{res}}$ and write a generalized modulation force as a sum $\sum_k 2\Gamma_k \cos(2\Omega_k t + \phi_k) q_k$. Assuming spectrally resolved detection of all quadratures, the set of modulation phases can be extracted and used for the periodic adjustment of the modulation force at intervals multiples of $\delta\tau$. The results are presented in Figs. 5(a) and 5(c) for the case of equidistant, well-separated $n_{\text{res}} = 8$ resonances and in Figs. 5(b) and 5(d) for the particular case where two modes are close to degeneracy. The final occupancy in the steady state is calculated for individual, isolated cooling (ignoring the presence of adjacent resonances) as black stars and then compared with the performance of the simultaneous cooling technique as blue triangles. The red dots show the initial occupancy of each mode. The results are consistent with previous treatments of cold-damping [21,22], showing that cooling is efficient as long as the modes are frequency-separated by more than the effective cooling rate Γ_k . This is further exemplified in Fig. 5(c) where the cooling dynamics for all modes is presented with the clear message of Fig. 5(d) that the two adjacent modes are unaffected by the cooling mechanism.

V. TOWARDS THE QUANTUM LIMIT

Let us now estimate the efficiency of the phase adaptive scheme close to the quantum ground state, where quantum fluctuations in the detected quadratures can play a crucial role. Since numerical computations for large temperature initial states are inefficient, owing to the large size of the Hilbert space, we focus on identifying the role of quantum uncertainty at the analytical level and numerically analyze the feasibility

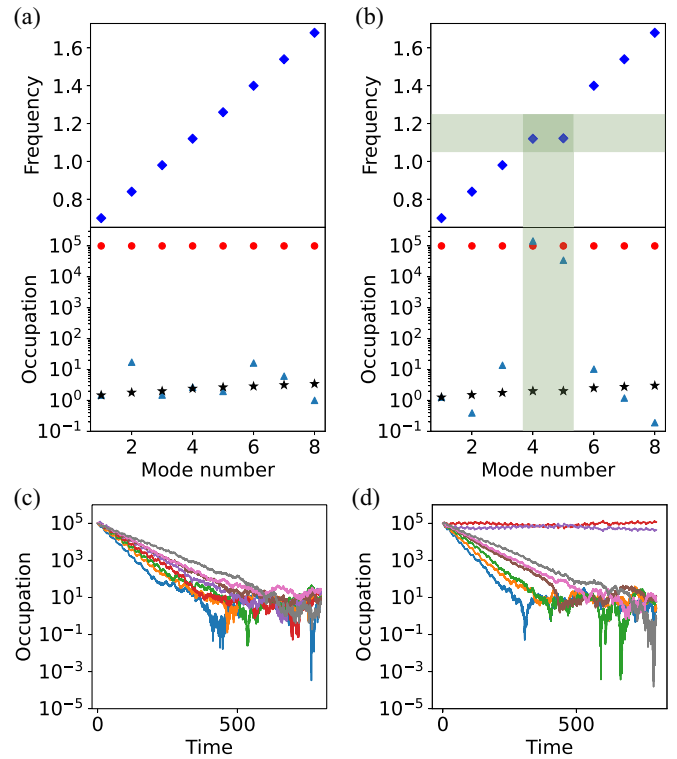


FIG. 5. Simultaneous cooling. (a) Final occupancy (lower panel, red dots: initial occupancy, black stars: isolated cooling, blue triangles: simultaneous cooling) of eight equidistant modes (upper panel). (b) Same as in (a) but considering the case where two modes are degenerate in frequency. (c) Time dynamics of the cooling process for all modes showing fluctuations associated with the competition between the imposed cooling and the inherent heating dynamics owed to the thermal bath. (d) Same as in (c) but with the clear message that degenerate modes are decoupled from the cooling dynamics. The parameters are chosen as $\gamma/\Omega = 10^{-6}$, $b = 0.05$ and the initial occupancy is close to 10^5 for all modes. The time is expressed in inverse units of Ω .

of mitigating the effect of parametric amplification of quantum noise fluctuations close to zero occupancy, where the size of the Hilbert space necessary for the convergence of numerical simulations is considerably reduced.

The exact numerical simulations in the reduced size Hilbert space are shown in Fig. 6(a) where we follow the dynamics of an initially low-temperature oscillator subject to phase adaptive feedback. We find that an increase in the feedback steps manages to keep the oscillator in a low temperature by fighting against the amplification of fluctuations stemming from the parametric nature of the drive. However, residual occupancies at the order of a few phonons cannot be avoided. This can be explained by inspection of Eq. (13): we model the effect of quantum fluctuations by adding a normal distribution random variable $\mathcal{N}(0, 1)$ to the detected quadratures. For large oscillation amplitudes where q_0 and p_0 assume large values, the uncertainty $\mathcal{N}(0, 1)$ does not have much effect on the estimate of the optimal phase. Close to the ground state, where the averages are close to zero, the quantum uncertainty renders the optimal phase estimate quasirandom, therefore providing no cooling or even a heating effect.

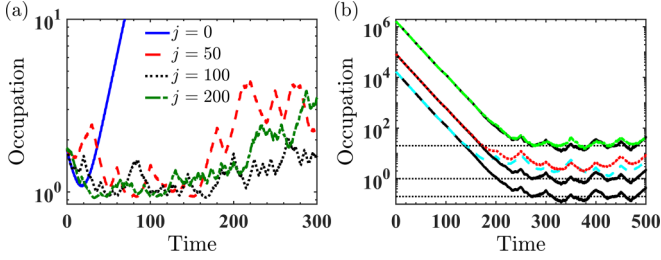


FIG. 6. Performance in the quantum regime. (a) Occupancy of a quantum oscillator starting in a low-temperature state in the absence of phase feedback (blue solid line, which shows immediate quick amplification of quantum fluctuations) and with increasing feedback steps ($j = 50, 100, 200$). The simulations are performed in a Hilbert space with dimension 10^2 by following the evolution of operators written as matrices in the Fock basis. (b) Numerical simulations showing final occupancies for trajectories corresponding to increasing initial occupancies from 10^4 to 5×10^4 to 10^6 . The black solid lines show the ideal case without quantum fluctuations but including thermal ones. For $n_{\text{th}} = 10^6$ the simulation including quantum fluctuations in the detected quadratures (green, dotted) shows similar behavior with final occupancy at the level of 20 phonons. For lower n_{th} the imperfect detection process (red, dotted for 5×10^4 and cyan, dashed for 10^4) leads to a saturation quite far from the classically predicted results at the level of a few residual phonons. Numerical simulations are performed by assuming that quantum fluctuations are included in the detection process and subsequently in the estimate of the feedback phase.

We can extend this observation and numerically investigate the dynamics for the higher initial temperature case by simply including the quantum fluctuations in the detected optimal phase similar to the case of the measurement imperfection as normal distributions $\mathcal{N}(0, 1)$ in each quadrature. Results are presented in Fig. 6(b) showing that, for the initial stages, the phase adaptive techniques leads to efficient exponential cooling with the theoretically predicted cooling rate Γ . At later stages, for situations where the predicted final occupancies are large, as in the example where $n_{\text{th}} = 10^6$, the quantum fluctuations do not play any role and the cooling is still efficient. However, for initial conditions such as $n_{\text{th}} = 10^4$ or $n_{\text{th}} = 5 \times 10^4$, where classical averages at longer times are at the order of the values picked from the distribution $\mathcal{N}(0, 1)$, the estimated optimal phase acquires a large uncertainty, leading to a saturation at the level of a few phonons. Reheating is, however, prohibited as the feedback becomes again efficient as soon as the system acquires larger classical amplitudes.

Let us now consider an approximate, phenomenological model where we assume that the system reaches quasiequilibrium between two consecutive applications of the phase feedback at a few phonon occupancy with a measurement imprecision modified cooling rate $\bar{\Gamma}$. This allows to estimate the final occupancy (see Appendix C) from the variance in the position quadrature

$$\langle \hat{q}^2 \rangle = \frac{\gamma(\bar{\Gamma} + \gamma \sin \phi)}{\bar{\Gamma}^2 - \gamma^2} \left(n_{\text{th}} + \frac{1}{2} \right) + \frac{\bar{\Gamma}(\bar{\Gamma} + \gamma \sin \phi)}{2(\bar{\Gamma}^2 - \gamma^2)}. \quad (17)$$

The first contribution describes cooling, while the second term is necessary to secure a larger than $1/2$ variance stemming from quantum fluctuations. For large initial occupancies,

where $\bar{\Gamma}$ is well approximated by Γ , the analytical expression leads to a final occupancy $n_{\text{final}} = \gamma/\Gamma(n_{\text{th}} + 1/2)$ showing a reduction by a factor of Γ/γ . For cases of reduced initial occupancies where the system gets closer to the ground state, an analytical estimate is not possible and numerical simulations show that the residual occupancies is at the order of a few phonons as witnessed in Fig. 6(b).

VI. DISCUSSIONS AND OUTLOOK

In contrast to prior designs of parametric feedback [30] of parametric cooling [25], we consider a pure actuation on the phase of the feedback. The main benefit is that the predicted dynamics is purely exponential in energy loss (for initial stages where large occupancies are assumed) and can be captured in an analytical model which identifies the knobs allowing for the cooling solution to dominate at any times. Use of pure phase actuation has additional technical benefits: extraneous heating from direct modulation of the radiation pressure force can lead to extraneous (ohmic) heating, which can be absent for pure phase modulation. While parametric cooling has been experimentally introduced for the control of optically levitated particles [25,26], atoms in cavities [27] or nanoelectromechanical resonators [28], our description generally involves solely the modulation of the spring constant of the resonator. Therefore, applications could extend beyond standard optomechanical systems, such as a membrane-in-the-middle optomechanical systems, to the refrigeration of phonon modes in solid-state systems. As numerical simulations are computationally challenging, we leave the problem of analyzing and optimizing the feedback in the regime of low occupancy for future studies employing quantum trajectory techniques [34,38].

Note added. The authors became aware of a related paper by Manikandan *et al.* [39], where an alternative treatment derived the same phase relation as that found here and also considered the role of squeezing arising from the parametric modulations of the trapping potential.

ACKNOWLEDGMENTS

We acknowledge financial support from the Max Planck Society and the Deutsche Forschungsgemeinschaft (DFG, German Research Foundation) Project-ID No. 429529648-TRR 306 QuCoLiMa (“Quantum Cooperativity of Light and Matter”).

APPENDIX A: MODELING BY WIENER PROCESS FOR UNDERDAMPED OSCILLATORS

To numerically model the influence of the thermal environment on a harmonically bound particle, we rewrite the coupled difference equations for an undriven harmonic oscillator

$$dq = \Omega p dt, \quad (A1)$$

$$dp = -\gamma p dt - \Omega q dt + \sqrt{2\gamma n_{\text{th}}} dW(t), \quad (A2)$$

where $dW(t)$ is a Wiener process as described in the main text. Note that, unlike a free particle [40], there is no asymptotic

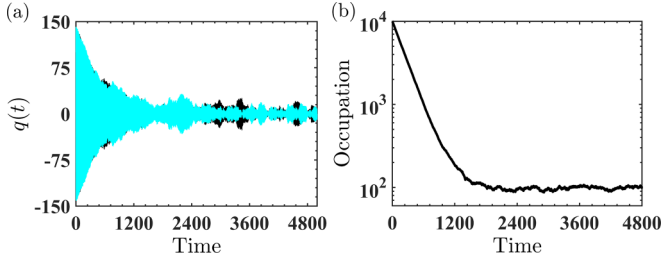


FIG. 7. Thermalization of an initially hot mechanical oscillator. (a) Time evolution of the two position trajectories. (b) Average occupancy as a function of time. The parameters are $\gamma = 4 \times 10^{-3}\Omega$ and $n_{\text{th}} = 100$.

diffusion for a particle subjected to a harmonic potential [41]. In fact in the later case, both the position and momentum attain an equilibrium distribution. This means that in the steady state the mechanical oscillator should thermalize with the environment. To check this numerically, we simulate Eqs. (A1) and (A2) in the underdamped case and using Wiener increments [34], which are Gaussian with a variance equal to numerical time step dt . We begin with an initially hot mechanical oscillator damped at a rate $\gamma = 4 \times 10^{-3}\Omega$ by a thermal environment of effective occupancy $n_{\text{th}} = 100$. The resulting thermalization of the mechanical oscillator is shown in Fig. 7. An initially hot mechanical system follows the time evolution provided by the thermal environment [Fig. 7(a)] and in the steady state the average occupancy approaches $n_{\text{th}} = 100$ [Fig. 7(b)], as expected.

APPENDIX B: CLASSICAL STOCHASTIC EVOLUTION

The coupled difference equations

$$dq = \Omega p dt, \quad (\text{B1a})$$

$$dp = -\gamma p dt - \Omega q dt + \mathcal{F}_{\text{mod}} dt + \sqrt{2\gamma n_{\text{th}}} dW(t), \quad (\text{B1b})$$

can be directly numerically simulated by modeling $dW(t) = \sqrt{dt}\mathcal{N}(0, 1)$, where $\mathcal{N}(0, 1)$ describes a normally distributed random variable of unit variance. However, more analytical insight can be obtained by turning the difference equations into a set of recurrence equations. We discretize the time interval $[0, t]$ into n steps of duration $dt = t/n$ and can then rewrite the equations above as

$$\mathbf{v}_n - \mathcal{M}_n \mathbf{v}_{n-1} = \sqrt{2\gamma n_{\text{th}}} \mathbf{u} dW_n, \quad (\text{B2})$$

where $\mathbf{v} = (q, p)^\top$ and $\mathbf{u} = (0, 1)^\top$ and the evolution matrix is defined as

$$\mathcal{M}_n = \begin{bmatrix} 1 & \Omega dt \\ -\Omega dt + 2\Gamma \cos[2\Omega(n-1)dt + \phi] dt & 1 - \gamma dt \end{bmatrix}. \quad (\text{B3})$$

A solution can be then found easily and can be written in terms of time-ordered matrices $\mathcal{T}_{nj} = \mathcal{M}_n \mathcal{M}_{n-1} \dots \mathcal{M}_j$ in the

following form:

$$\mathbf{v}_n = \mathcal{T}_{n1} \mathbf{v}_0 + \sqrt{2\gamma n_{\text{th}}} \sum_{j=1}^{n-1} \mathcal{T}_{nj} \mathbf{u} dW_{n-j}. \quad (\text{B4})$$

As a simple check, let us describe solely the thermalization dynamics of an unmodulated oscillator (setting $\Gamma = 0$). The time-ordered matrices are much simpler now: $\mathcal{T}_{n1} = \mathcal{M}^n$ and $\mathcal{T}_{nj} = \mathcal{M}^{n-j}$. Under the assumption that $\gamma \ll \Omega$, diagonalization of the matrix $\mathcal{M} = S\Lambda S^{-1}$ is straightforward in terms of the two eigenvalues of \mathcal{M} equal to $\lambda_1 = 1 - \gamma dt/2 - i\Omega dt$, $\lambda_2 = 1 - \gamma dt/2 + i\Omega dt$. Notice that the two eigenvalues can be rewritten as $\lambda_1 = (1 - \gamma dt/2)e^{-i\Omega dt} = re^{i\theta}$ and $\lambda_2 = re^{-i\theta}$ where $r = 1 - \gamma t/2n$ and $\theta = \Omega t/n$. The resulting quadratures after n steps are written as

$$q_n = \frac{\lambda_1^n + \lambda_2^n}{2} q_0 + i \frac{\lambda_1^n - \lambda_2^n}{2} p_0 + \sqrt{2\gamma n_{\text{th}}} \sum_{j=0}^{n-1} \frac{\lambda_1^j - \lambda_2^j}{2} dW_j, \quad (\text{B5a})$$

$$p_n = \frac{\lambda_1^n + \lambda_2^n}{2} p_0 - i \frac{\lambda_1^n - \lambda_2^n}{2} q_0 + \sqrt{2\gamma n_{\text{th}}} \sum_{j=0}^{n-1} \frac{\lambda_1^j + \lambda_2^j}{2} dW_j, \quad (\text{B5b})$$

where the deterministic parts describe simply the oscillatory weakly damped transient evolution and the last terms are the effect of the thermal environment. In the large n limit we find a closed expression

$$q(t) = e^{-\gamma t/2} [q_0 \cos(\Omega t) + p_0 \sin(\Omega t)] + \lim_{n \rightarrow \infty} \sqrt{2\gamma n_{\text{th}}} \sum_{j=0}^{n-1} r^j \sin(j\theta) dW_j, \quad (\text{B6a})$$

$$p(t) = e^{-\gamma t/2} [p_0 \cos(\Omega t) - q_0 \sin(\Omega t)] + \lim_{n \rightarrow \infty} \sqrt{2\gamma n_{\text{th}}} \sum_{j=0}^{n-1} r^j \cos(j\theta) dW_j, \quad (\text{B6b})$$

where we use that $\lim_{n \rightarrow \infty} (1 - \gamma t/2n)^n = e^{-\gamma t/2}$. From these expressions, we can estimate that in steady state $\langle q^2 \rangle_{\text{ss}} = \langle p^2 \rangle_{\text{ss}} = n_{\text{th}}$ by using $\langle dW_j dW_{j'} \rangle = \delta_{jj'} dt/n$ and evaluating the limit $\lim_{n \rightarrow \infty} \sum_{j=0}^{n-1} r^{2j} \sin^2(j\theta) = 1/(2\gamma t)$.

APPENDIX C: TOWARDS THE QUANTUM LIMIT

Let us assume a steady state and fix the modulation phase to ϕ such that the cooling rate is exponential at rate $\bar{\Gamma}$ (with the maximum value Γ for optimal feedback and close to zero when fluctuations dominate) and both the position and momentum expectation values vanish. We will compute the final occupancy from the variance in position (assuming thermal equipartition between momentum and position quadratures) obtained from the power spectrum in the Fourier domain $S_q(\omega)$ via an integration $\langle \hat{q}^2 \rangle = 1/(2\pi) \int_{-\infty}^{\infty} d\omega S_q(\omega)$. The

Fourier-transformed equations read

$$-i\omega\hat{q}(\omega) = \Omega\hat{p}(\omega), \quad (\text{C1a})$$

$$\begin{aligned} -i\omega\hat{p}(\omega) &= -\gamma\hat{p}(\omega) - \Omega\hat{q}(\omega) \\ &+ \bar{\Gamma}[e^{i\phi}\hat{q}(\omega - 2\Omega) + e^{-i\phi}\hat{q}(\omega + 2\Omega)] + \hat{\zeta}(\omega). \end{aligned} \quad (\text{C1b})$$

Notice that, for $\bar{\Gamma} = 0$, the above equations lead to $\hat{q}(\omega) = \chi(\omega)\hat{\zeta}(\omega)$ where the mechanical susceptibility is

$$\chi(\omega) = \frac{\Omega}{(\Omega^2 - \omega^2) - i\gamma\omega}. \quad (\text{C2})$$

This indicates a simple way of computing the variance by using the correlations of the thermal environment $\langle \zeta(\omega)\zeta(\omega') \rangle = S_\zeta(\omega)\delta(\omega + \omega')$ where $S_\zeta(\omega)$ is the thermal power spectrum with sidebands $S_\zeta(-\Omega) = 2\gamma n_{\text{th}}$ and $S_\zeta(\Omega) = 2\gamma(n_{\text{th}} + 1)$. As for very high mechanical quality factors $Q_m \gg 1$, the susceptibility is a very sharply peaked function around $\pm\Omega$ and we can approximate it around the two poles at $\pm\Omega$ by expanding it in terms of a small quantity $\gamma \ll |\Delta| \ll \Omega$. The expansion is then $\chi(-\Omega + \Delta) \simeq 1/(2\Delta + i\gamma)$ and $\chi(+\Omega + \Delta) \simeq 1/(-2\Delta - i\gamma)$. The variance can then be approximated by $\langle \hat{q}^2 \rangle(t) = 1/(2\pi) \int_{-\infty}^{\infty} d\Delta (4\Delta^2 + \gamma^2)^{-1} [S_\zeta(-\Omega) + S_\zeta(\Omega)] = n_{\text{th}} + 1/2$ as expected. We made use of the integral $1/(2\pi) \int_{-\infty}^{\infty} d\Delta 1/(4\Delta^2 + \gamma^2) = \pi/(2\gamma)$.

We can now rewrite Eqs. (C1) as a recursive equation

$$\begin{aligned} \hat{q}(\omega) &= \bar{\Gamma}\chi(\omega)[e^{i\phi}\hat{q}(-2\Omega + \omega) + e^{-i\phi}\hat{q}(2\Omega + \omega)] \\ &+ \chi(\omega)\hat{\zeta}(\omega). \end{aligned} \quad (\text{C3})$$

We then proceed as above, making small variations around $\pm\Omega$ and assuming that the only components which contribute to the power spectrum of the position quadrature are $\hat{q}(\pm\Omega + \Delta)$. We can now separate two coupled equations

$$\begin{aligned} \hat{q}(-\Omega + \Delta) &= \bar{\Gamma}\chi(-\Omega + \Delta)e^{-i\phi}\hat{q}(\Omega + \Delta) \\ &+ \chi(-\Omega + \Delta)\hat{\zeta}(-\Omega + \Delta), \end{aligned} \quad (\text{C4a})$$

$$\begin{aligned} \hat{q}(\Omega + \Delta) &= \bar{\Gamma}\chi(\Omega + \Delta)e^{i\phi}\hat{q}(-\Omega + \Delta) \\ &+ \chi(\Omega + \Delta)\hat{\zeta}(\Omega + \Delta), \end{aligned} \quad (\text{C4b})$$

and invert them to find the solutions for $q(-\Omega + \Delta)$ and $q(\Omega + \Delta)$ expressed as

$$\begin{aligned} \hat{q}(-\Omega + \Delta) &= -\bar{\chi}(\Delta)[-(2\Delta + i\gamma)\zeta(-\Omega + \Delta) \\ &+ \bar{\Gamma}e^{-i\phi}\zeta(\Omega + \Delta)], \end{aligned} \quad (\text{C5a})$$

$$\begin{aligned} \hat{q}(\Omega + \Delta) &= -\bar{\chi}(\Delta)[\bar{\Gamma}e^{i\phi}\zeta(-\Omega + \Delta) \\ &+ (2\Delta + i\gamma)\zeta(\Omega + \Delta)]. \end{aligned} \quad (\text{C5b})$$

The modified mechanical susceptibility is approximated by the following expression (under the assumption that $|\Delta| \ll \Omega$):

$$\bar{\chi}(\Delta) = \frac{1}{4\Delta^2 + \bar{\Gamma}^2 - \gamma^2 + 4i\gamma\Delta}. \quad (\text{C6})$$

The denominator shows the presence of the optical damping rate $\bar{\Gamma}$ but not as a broadening adding to γ as is the case for cold damping or cavity cooling. We now again use the correlations of the noise term in the frequency

domain, however supplemented with the bath responsible with damping at rate Γ and with zero temperature. Notice that, for small Δ , the only contributing terms are $\langle \zeta(-\Omega + \Delta)\zeta(\Omega + \Delta') \rangle \simeq S(-\Omega)\delta(\Delta + \Delta')$ and $\langle \zeta(\Omega + \Delta)\zeta(-\Omega + \Delta') \rangle \simeq S(\Omega)\delta(\Delta + \Delta')$ where now $S(-\Omega) = 2\gamma n_{\text{th}}$ and $S(\Omega) = 2\gamma(n_{\text{th}} + 1) + 2\Gamma$. This leads to the following contributions:

$$\begin{aligned} &\langle \hat{q}(-\Omega + \Delta)\hat{q}(-\Omega + \Delta') \rangle \\ &= |\bar{\chi}(\Delta)|^2 \bar{\Gamma} e^{-i\phi} \{ 2\Delta [S(\Omega) \\ &- S(-\Omega)] - i\gamma [S(-\Omega) + S(\Omega)] \} \delta(\Delta + \Delta'), \end{aligned} \quad (\text{C7a})$$

$$\begin{aligned} &\langle \hat{q}(\Omega + \Delta)\hat{q}(\Omega + \Delta') \rangle \\ &= |\bar{\chi}(\Delta)|^2 \bar{\Gamma} e^{i\phi} \{ 2\Delta [S(\Omega) \\ &- S(-\Omega)] + i\gamma [S(-\Omega) + S(\Omega)] \} \delta(\Delta + \Delta'), \end{aligned} \quad (\text{C7b})$$

$$\begin{aligned} &\langle \hat{q}(-\Omega + \Delta)\hat{q}(\Omega + \Delta') \rangle \\ &= |\bar{\chi}(\Delta)|^2 \{ [4\Delta^2 + \gamma^2] S(-\Omega) \\ &+ \bar{\Gamma}^2 S(\Omega) \} \delta(\Delta + \Delta'), \end{aligned} \quad (\text{C7c})$$

$$\begin{aligned} &\langle \hat{q}(\Omega + \Delta)\hat{q}(-\Omega + \Delta') \rangle \\ &= |\bar{\chi}(\Delta)|^2 \{ \bar{\Gamma}^2 S[-\Omega] \\ &+ (4\Delta^2 + \gamma^2) S(\Omega) \} \delta(\Delta + \Delta'). \end{aligned} \quad (\text{C7d})$$

We can now add all the contributions to find the position power spectrum via the following integral:

$$\begin{aligned} \langle \hat{q}^2 \rangle &= \frac{1}{2\pi} \int_{-\infty}^{\infty} d\Delta |\bar{\chi}(\Delta)|^2 \left\{ 4\gamma(2\gamma\bar{\Gamma}\sin\phi + 4\Delta^2 + \bar{\Gamma}^2 \right. \\ &+ \gamma^2) \left(n_{\text{th}} + \frac{1}{2} \right) + 2\bar{\Gamma}(4\Delta(\gamma + \bar{\Gamma})\cos\phi + 2\gamma\bar{\Gamma}\sin\phi \\ &+ 4\Delta^2 + \bar{\Gamma}^2 + \gamma^2) \left. \right\} \end{aligned} \quad (\text{C8})$$

The result for the relevant case $\bar{\Gamma} > \gamma$ is

$$\langle \hat{q}^2 \rangle = \frac{\gamma(\bar{\Gamma} + \gamma\sin\phi)}{\bar{\Gamma}^2 - \gamma^2} \left(n_{\text{th}} + \frac{1}{2} \right) + \frac{\bar{\Gamma}(\bar{\Gamma} + \gamma\sin\phi)}{2(\bar{\Gamma}^2 - \gamma^2)}. \quad (\text{C9})$$

Notice that in the limit where the additional damping dominates $\bar{\Gamma} \gg \gamma$ we can simplify the expression above and compute the final occupancy $n_{\text{final}} = \langle \hat{q}^2 \rangle - 1/2$ to lead to

$$n_{\text{final}} = \frac{\gamma}{\bar{\Gamma}} \left(n_{\text{th}} + \frac{1}{2} \right). \quad (\text{C10})$$

In the opposite case where $\bar{\Gamma} < \gamma$ the variance reads

$$\langle \hat{q}^2 \rangle = \frac{\gamma(\gamma + \bar{\Gamma}\sin\phi)}{\gamma^2 - \bar{\Gamma}^2} \left(n_{\text{th}} + \frac{1}{2} \right) + \frac{\bar{\Gamma}(\gamma + \bar{\Gamma}\sin\phi)}{2(\gamma^2 - \bar{\Gamma}^2)}. \quad (\text{C11})$$

For $\bar{\Gamma} = 0$ we recover the expected result $\langle \hat{q}^2 \rangle = n_{\text{th}} + 1/2$.

APPENDIX D: EFFECT OF CANONICAL NOISE

To properly account for noise in optomechanical systems, one usually makes use of the Brownian noise model, which

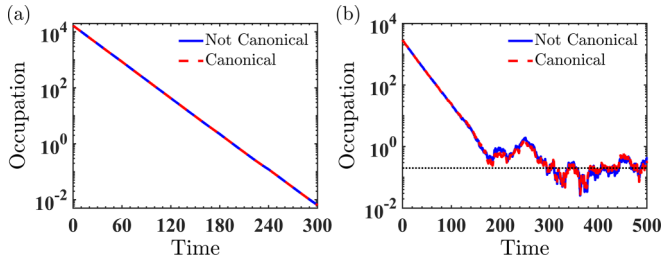


FIG. 8. Effect of the canonical noise on the dynamics of the mechanical oscillator. (a) Occupancy (without noise) obtained by solving Eqs. 1(a) and 1(b) of the main text (solid blue line) and Eqs. (D1) and (D2) (dashed red line). (b) Sample trajectories in the absence (solid blue line) and presence (dashed red line) of canonical noise. Parameters are same as used in Fig. 4.

can be seen as an average over the infinite number of small kicks stemming from the environment. This then leads to a stochastic force and damping in the momentum quadrature while the position quadrature is unaffected. The resulting spectrum of the force is not flat but instead described by colored noise, and generally the correlations of the noise in the time domain deviate from a delta function by the addition of a derivative of a delta function. However, as is the case for high-quality mechanical oscillators of small frequency

$\hbar\Omega \ll k_B T_{\text{th}}$, an approximation by a flat spectrum and thus delta correlation is very accurate. This also allows one to study the dynamics of the system in terms of bosonic annihilation $[\hat{b} = (\hat{q} + i\hat{p})/\sqrt{2}]$ and creation $[\hat{b}^\dagger = (\hat{q} - i\hat{p})/\sqrt{2}]$ operators and the mechanical loss can be introduced via a Lindblad term with a collapse operator b and decay rate γ (canonical noise). Let us analyze this kind of model by noticing that the equations of motion are now modified and noise is present in both quadratures

$$\dot{q} = \Omega p - \frac{\gamma}{2} q + \sqrt{\gamma(n_{\text{th}} + 1/2)} q_{\text{in}}, \quad (\text{D1})$$

$$\dot{p} = -\Omega q - \frac{\gamma}{2} p + 2\Gamma \cos(2\Omega t + \phi) q + \sqrt{\gamma(n_{\text{th}} + 1/2)} p_{\text{in}}, \quad (\text{D2})$$

where $q_{\text{in}}(t)$ and $p_{\text{in}}(t)$ are delta-correlated canonical noise contributions. Using the above equations, we simulate the dynamics and compare it with the dynamics obtained by using the Brownian noise model. The results are shown to be perfectly in agreement in Fig. 8(a) (for noiseless trajectories where only the predicted cooling rate is important) and for noisy trajectories in Fig. 8(b), where the behavior close to the final cooled state clearly shows the equivalence of the two noise models.

-
- [1] G. Anetsberger, O. Arcizet, Q. P. Unterreithmeier, R. Rivière, A. Schliesser, E. M. Weig, J. P. Kotthaus, and T. J. Kippenberg, Near-field cavity optomechanics with nanomechanical oscillators, *Nat. Phys.* **5**, 909 (2009).
- [2] F. Fogliano, B. Besga, A. Reigue, L. Mercier de Lépinay, P. Heringlake, C. Gouriou, E. Eyraud, W. Wernsdorfer, B. Pigeau, and O. Arcizet, Ultrasensitive nano-optomechanical force sensor operated at dilution temperatures, *Nat. Commun.* **12**, 4124 (2021).
- [3] A. G. Krause, M. Winger, T. D. Blasius, Q. Lin, and O. Painter, A high-resolution microchip optomechanical accelerometer, *Nat. Photonics* **6**, 768 (2012).
- [4] M. Sansa, M. Defoort, A. Brenac, M. Hermouet, L. Banniard, A. Fafin, M. Gely, C. Masselon, I. Favero, G. Jourdan, and S. Hentz, Optomechanical mass spectrometry, *Nat. Commun.* **11**, 3781 (2020).
- [5] L. Diósi, A universal master equation for the gravitational violation of quantum mechanics, *Phys. Lett. A* **120**, 377 (1987).
- [6] R. Penrose, On gravity's role in quantum state reduction, *Gen. Relativ. Gravit.* **28**, 581 (1996).
- [7] W. Marshall, C. Simon, R. Penrose, and D. Bouwmeester, Towards Quantum Superpositions of a Mirror, *Phys. Rev. Lett.* **91**, 130401 (2003).
- [8] O. Romero-Isart, A. C. Pflanzer, F. Blaser, R. Kaltenbaek, N. Kiesel, M. Aspelmeyer, and J. I. Cirac, Large Quantum Superpositions and Interference of Massive Nanometer-Sized Objects, *Phys. Rev. Lett.* **107**, 020405 (2011).
- [9] M. Aspelmeyer, T. J. Kippenberg, and F. Marquardt, Cavity optomechanics, *Rev. Mod. Phys.* **86**, 1391 (2014).
- [10] U. Delić, M. Reisenbauer, D. Grass, N. Kiesel, V. Vuletić, and M. Aspelmeyer, Cavity Cooling of a Levitated Nanosphere by Coherent Scattering, *Phys. Rev. Lett.* **122**, 123602 (2019).
- [11] U. Delić, M. Reisenbauer, K. Dare, D. Grass, V. Vuletić, N. Kiesel, and M. Aspelmeyer, Cooling of a levitated nanoparticle to the motional quantum ground state, *Science* **367**, 892 (2020).
- [12] D. Windey, C. Gonzalez-Ballester, P. Maurer, L. Novotny, O. Romero-Isart, and R. Reimann, Cavity-Based 3D Cooling of a Levitated Nanoparticle via Coherent Scattering, *Phys. Rev. Lett.* **122**, 123601 (2019).
- [13] C. Gonzalez-Ballester, P. Maurer, D. Windey, L. Novotny, R. Reimann, and O. Romero-Isart, Theory for cavity cooling of levitated nanoparticles via coherent scattering: Master equation approach, *Phys. Rev. A* **100**, 013805 (2019).
- [14] T. Li, S. Kheifets, and M. G. Raizen, Millikelvin cooling of an optically trapped microsphere in vacuum, *Nat. Phys.* **7**, 527 (2011).
- [15] J. Millen, T. S. Monteiro, R. Pettit, and A. N. Vamivakas, Optomechanics with levitated particles, *Rep. Prog. Phys.* **83**, 026401 (2020).
- [16] M. Rossi, D. Mason, J. Chen, Y. Tsaturyan, and A. Schliesser, Measurement-based quantum control of mechanical motion, *Nature (London)* **563**, 53 (2018).
- [17] F. Tebbenjohanns, M. L. Mattana, M. Rossi, M. Frimmer, and L. Novotny, Quantum control of a nanoparticle optically levitated in cryogenic free space, *Nature (London)* **595**, 378 (2021).
- [18] L. Magrini, P. Rosenzweig, C. Bach, A. Deutschmann-Olek, S. G. Hofer, S. Hong, N. Kiesel, A. Kugi, and M. Aspelmeyer, Real-time optimal quantum control of mechanical motion at room temperature, *Nature (London)* **595**, 373 (2021).
- [19] C. Whittle *et al.*, Approaching the motional ground state of a 10-kg object, *Science* **372**, 1333 (2021).
- [20] L. Dania, D. S. Bykov, M. Knoll, P. Mestres, and T. E. Northup, Optical and electrical feedback cooling of a silica nanoparticle levitated in a paul trap, *Phys. Rev. Res.* **3**, 013018 (2021).

- [21] C. Sommer and C. Genes, Partial Optomechanical Refrigeration via Multimode Cold-Damping Feedback, *Phys. Rev. Lett.* **123**, 203605 (2019).
- [22] C. Sommer, A. Ghosh, and C. Genes, Multimode cold-damping optomechanics with delayed feedback, *Phys. Rev. Res.* **2**, 033299 (2020).
- [23] C. Genes, D. Vitali, P. Tombesi, S. Gigan, and M. Aspelmeyer, Ground-state cooling of a micromechanical oscillator: Comparing cold damping and cavity-assisted cooling schemes, *Phys. Rev. A* **77**, 033804 (2008).
- [24] K. Komori, D. Ďurovčiková, and V. Sudhir, Quantum theory of feedback cooling of an anelastic macromechanical oscillator, *Phys. Rev. A* **105**, 043520 (2022).
- [25] J. Gieseler, B. Deutsch, R. Quidant, and L. Novotny, Subkelvin Parametric Feedback Cooling of a Laser-Trapped Nanoparticle, *Phys. Rev. Lett.* **109**, 103603 (2012).
- [26] C. Gonzalez-Ballester, M. Aspelmeyer, L. Novotny, R. Quidant, and O. Romero-Isart, Levitodynamics: Levitation and control of microscopic objects in vacuum, *Science* **374**, eabg3027 (2021).
- [27] C. Sames, C. Hamsen, H. Chibani, P. A. Altin, T. Wilk, and G. Rempe, Continuous parametric feedback cooling of a single atom in an optical cavity, *Phys. Rev. A* **97**, 053404 (2018).
- [28] L. G. Villanueva, R. B. Karabalin, M. H. Matheny, E. Kenig, M. C. Cross, and M. L. Roukes, A nanoscale parametric feedback oscillator, *Nano Lett.* **11**, 5054 (2011).
- [29] J. Gieseler, L. Novotny, and R. Quidant, Thermal nonlinearities in a nanomechanical oscillator, *Nat. Phys.* **9**, 806 (2013).
- [30] B. Rodenburg, L. P. Neukirch, A. N. Vamivakas, and M. Bhattacharya, Quantum model of cooling and force sensing with an optically trapped nanoparticle, *Optica* **3**, 318 (2016).
- [31] D. Leibfried, R. Blatt, C. Monroe, and D. Wineland, Quantum dynamics of single trapped ions, *Rev. Mod. Phys.* **75**, 281 (2003).
- [32] I. Wilson-Rae, N. Nooshi, W. Zwerger, and T. J. Kippenberg, Theory of Ground State Cooling of a Mechanical Oscillator Using Dynamical Backaction, *Phys. Rev. Lett.* **99**, 093901 (2007).
- [33] F. Marquardt, J. P. Chen, A. A. Clerk, and S. M. Girvin, Quantum Theory of Cavity-Assisted Sideband Cooling of Mechanical Motion, *Phys. Rev. Lett.* **99**, 093902 (2007).
- [34] K. Jacobs, *Stochastic Processes for Physicists: Understanding Noisy Systems* (Cambridge University Press, Cambridge, England, 2010).
- [35] I. Brandão, D. Tandeitnik, and Guerreiro T, Coherent scattering-mediated correlations between levitated nanospheres, *Quantum Sci. Technol.* **6**, 045013 (2021).
- [36] H. Rudolph, K. Hornberger, and B. A. Stickler, Entangling levitated nanoparticles by coherent scattering, *Phys. Rev. A* **101**, 011804(R) (2020).
- [37] A. K. Chauhan, O. Černotík, and R. Filip, Stationary gaussian entanglement between levitated nanoparticles, *New J. Phys.* **22**, 123021 (2020).
- [38] K. Jacobs, *Quantum Measurement Theory and its Applications* (Cambridge University Press, Cambridge, England, 2014).
- [39] S. K. Manikandan and S. Qvarfort, Optimal quantum parametric feedback cooling, *Phys. Rev. A* **107**, 023516 (2023).
- [40] A. Papoulis and S. Pillai, *Probability, Random Variables, and Stochastic Processes*, McGraw-Hill Series in Electrical and Computer Engineering, (McGraw-Hill, New York, 2002).
- [41] V. Balakrishnan, *Elements of Nonequilibrium Statistical Mechanics* (Springer, New York, 2020).